1. The Influence of the Human Body on Electric and Magnetic Field Components in the Immediate Vicinity of the Body

Martin Schallner, Jan Waldmann, Stefan Hübner, Friedrich Landstorfer,
Institut für Hochfrequenztechnik, Universität Stuttgart,
Helmut Keller, Rainer Bitzer, Wandel & Goltermann

Abstract:
Warning devices and meters are necessary for personal safety in radio frequency (RF) and microwave electromagnetic fields. The relevant standards and guidelines dictate that the respective field strength must be displayed that would exist if no one were present in the field. Accordingly, we must first determine to what extent the presence of a human body influences the individual electric and magnetic field components. Extensive computer-based computations were performed to this end. With the results obtained, a field strength meter for personal safety applications was developed which exhibits significant advantages over previous solutions.

Keywords:
Field strength meter / Environmental electromagnetic compatibility (EEMC) / Measurement accuracy / Human body

1. Introduction

The standards and guidelines for personal safety in radio frequency (RF) and microwave electromagnetic fields dictate that the electric and magnetic field strength to which a person is exposed must exceed certain frequency-dependent limits. The field strengths must be determined in the absence of the person, or alternatively, a field strength meter must display the same field strength results whether it is situated in a free field or carried on the person. Consequently, it has to be determined to what extent the individual field strength components are influenced by the presence of the human body [1]. The Institut für Hochfrequenztechnik at the University of Stuttgart has developed various human body models for the FEKO simulation program which served as our tools in the frequency range from 100 kHz to 3 GHz. The models have more or less the geometric structure of a standing grown-up person with the arms at the sides or bent.

2. Pre-Observations on Modelling the Human Body

In order to compute the electric and magnetic fields which exist in the vicinity of the body when different waves are incident upon it, we must first develop an appropriate model for the body. As a first approximation, we use a highly simplified model to simulate the body i.e. a dielectric cuboid. Our computations assume a height of 170 cm, a width of 35 cm and a depth of 15 cm. With a relative dielectric constant of $\varepsilon_r = 50$ and a conductivity of $\sigma = 1$ S/m, the dielectric material corresponds to average human muscle tissue at lower frequencies.

The numerical computations were done using the FEKO program [2] utilizing the surface-current method. Here, the surface of the simulated body is broken down into small triangles and the boundary conditions on their surfaces are fulfilled with appropriate surface currents in the triangles.

Fig. 1 shows the segmented cuboid. The segmentation method chosen here breaks down the surface of the cuboid into 3312 triangles. However, finer segmentation is used in the immediate vicinity of the place of observation (chest height).

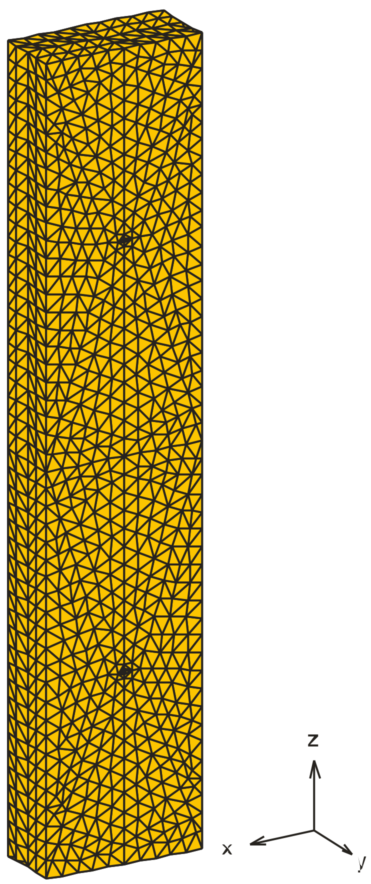

Fig. 1: FEKO simulation model for the dielectric cuboid

Computations of the electromagnetic field in and around the cuboid is limited to a maximum frequency of 350 MHz when utilizing an available working memory of 480 Mbytes and taking three planes of symmetry into account. In order to increase the maximum frequency we can compute, the cuboid must be broken into a higher number of segments which requires a still larger working memory. Consequently, the field conditions of interest can be determined only at relatively low frequencies even though the model is already highly simplified.

If we use a metallic model instead of a dielectric one for computing the field conditions in the vicinity of the body, the maximum computable frequency can significantly be

increased as the segmentation can be augmented by a factor of $\sqrt{\varepsilon_r} \approx 7$ while simultaneously the memory requirement per surface triangle is reduced by a factor of 4 [2].

With this technique, the field interference caused by the body is only slightly overemphasized and less than was initially suspected. This can be explained by the fact that the ideal metallic reflection has a reflection factor r_m = -1, while the incident wave still experiences a reflection factor $r_e \approx -0.75$ at the transition from the air into the medium of the body model with a relative dielectric constant of $\varepsilon_r = 50$. In other words, the results obtained using this technique are well suited for determining the worst case.

The following figures show the computed fields in front of the dielectric or metallic cuboid as a function of frequency with incidence of a vertically polarized planar wave propagating in the negative *y*-direction (see Fig. 1). All values given here are normalized to the amplitude of the incident wave. Two locations situated at chest height 3 cm and 100 cm in front of the cuboid are used as observation points. As could be expected from basic physics and was also confirmed through extensive computations, the effects of the cuboid on the incident wave are maximum for this excitation, which is why we do not consider any other excitation here.

The incident planar wave is vertically polarized and propagates in the negative *y*-direction and consequently offers an electric field strength component in the *z*-axis and a magnetic field strength component in the *x*-axis, only. At a frequency of about 60 MHz, the halfwave resonance of the cuboid comes into action. In this range, a pronounced *x*-component of the magnetic field strength and a *y*-component of the electric field strength occur, the latter not being contained in the incident wave. The halfwave resonance was also confirmed through measurements. Fig. 3 shows the electric and magnetic field strengths obtained from the sum of the squares of the respective components.

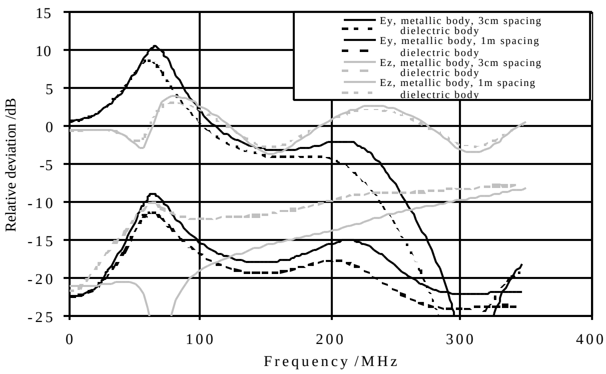

Fig. 2: Normalized y- and z-components of the electric field strength

Due to the strong reflection on the metallic or dielectric surface of the cuboid, a standing wave arises in the direction of the incident wave. As was expected, the amplitudes in front of the metallic cuboid are somewhat greater than in front of the dielectric one.

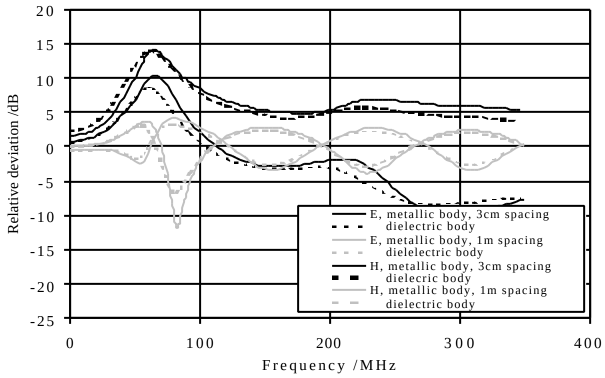

Fig 3: Normalized electric and magnetic field strength

A comparison between the field conditions in front of the metallic and dielectric cuboids shows that the metallic cuboid (which is much simpler in computational terms) characterizes the basic conditions very well. Based on this insight, our further research was restricted to metallic body models.

3. Body Model with Arms at the Sides

By modelling with a metallic surface, the maximum computable frequency increases significantly due to the less memory-extensive computation technique, while the detail of the model can be greatly increased at the same time.

The body model shown in **Fig. 4** with arms at the sides is 170 cm tall and enables computations up to a maximum frequency of 4 GHz due to the very fine segmentation with 4616 metallic triangles and utilization of two planes of symmetry.

The field conditions in front of the body were determined for the incidence of one planar wave in each case. Numerous propagation directions were investigated with horizontal and vertical polarization.

A point at chest height 3 cm in front of the body and laterally displaced by 7.5 cm is used as the observation site. This corresponds more or less to the region of a shirt pocket where a field strength warning device might be carried.

Figs. 5 and **6** illustrate the fields computed with FEKO in front of the body model shown in Fig. 4 as a function of frequency with incidence of a vertically or horizontally polarized planar wave propagating in the negative *y*-direction. Apart from the amplitudes of the electric field strength E and the magnetic field strength H, the amplitude of the normal component of the electric field strength E_n, which here corresponds to the *y*-component, and the amplitude of the tangential component of the magnetic field strength H_t, which here is formed from the sum of the squares of the *x*- and *y*-components, are also plotted. These two components do not disappear on the surface of the model in accordance with the boundary conditions.

As with the cuboid, the halfwave resonance is also clearly recognizable in the model with the arms at the sides upon incidence of a vertically polarized wave. This increases the electric as well as the magnetic field strength by up to 13.5 dB. However, due to the lower capacitive end loading, the resonant frequency has shifted towards a higher frequency and is now around 70 MHz.

Upon incidence of a horizontally polarized wave (see Fig. 6), a weak resonance occurs at about 100 MHz. This is due to the $\lambda/4$-resonance of the legs and can be largely eliminated by slightly damping the insides of the legs. For such excitation, the electric field strength at low frequencies is underestimated by about 6.5 dB.

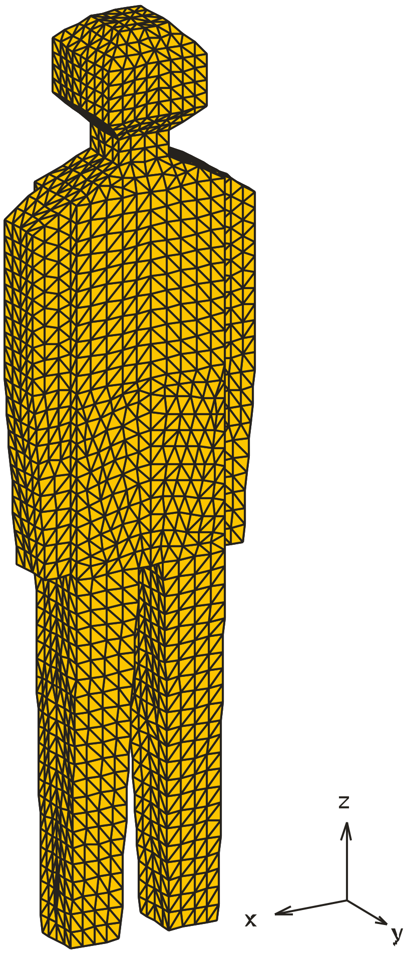

Fig. 4: FEKO simulation model for the body with arms at the side. The origin of the coordinate system is at the soles of the feet for the z-coordinate and in the center of the body for the x- and y-direction

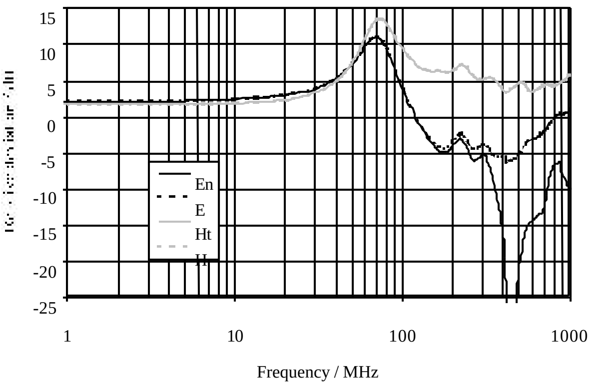

Fig. 5: Field conditions upon incidence of a vertically polarized wave propagating in the negative y-direction

This means that the only way to obtain the desired measurement accuracy is by evaluating the magnetic field strength.

Interestingly enough, at higher frequencies (starting at about 300 MHz) for both polarizations, the tangential electric field components are significantly larger than the normal ones. As a consequence the normal electric field component can not be

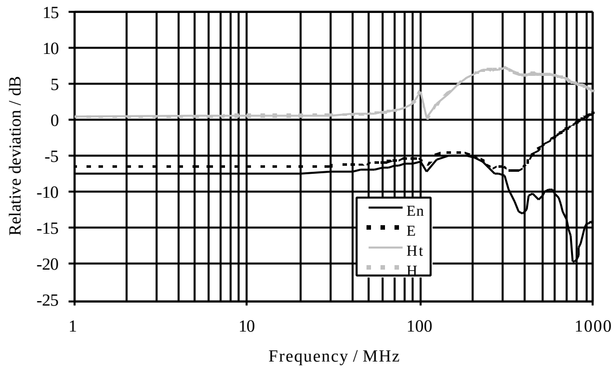

Fig. 6: Field conditions upon incidence of a horizontally polarized wave propagating in the negative y-direction

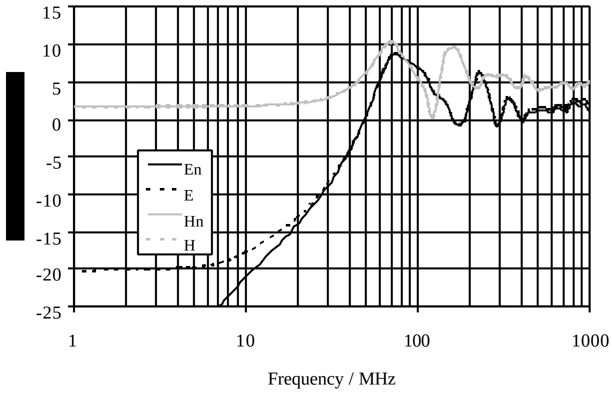

Fig. 7: Field conditions upon incidence of a vertically polarized wave propagating in the negative y-z-direction.

employed to monitor the safety limits using the electric field strength alone.

Full determination of the electric field strength requires an isotropic probe, however. Upon incidence of a vertically polarized wave propagating in the negative *y-z*-direction, i.e. incident at an angle of 45° diagonally from above on the front side of the body model, measurement of the electric field strength fails entirely at low frequencies as the tangential field component becomes larger than the normal component in this case as well. In other words, evaluation of the magnetic field strength at low frequencies cannot be avoided in this case.

If, on the other hand, a vertically polarized wave is laterally incident on the model (see **Fig. 8**), measurement of the magnetic field strength fails at low frequencies, making it necessary to evaluate the electric field strength for this direction of incidence.

The field conditions shown in Figs. 5-8 for frequencies below 1 GHz make it clear that the only way to reliably avoid underestimating the field exposure is by simultaneously measuring the electric and magnetic field strength.

For higher frequencies (e.g. above 1 GHz), the body essentially represents a surface that is not entirely reflective so that a standing wave arises in the direction of the incident wave. Arranging an absorber between the sensors and the body in order to reduce the influence of the standing wave significantly is therefore recommended. As was shown through actual

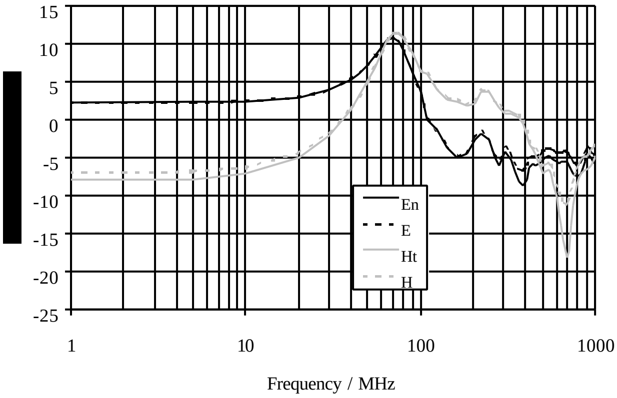

Fig. 8: Field conditions upon incidence of a vertically polarized wave propagating in the negative y-direction

measurements, this is a way of avoiding under- or overesti-estimating the exposure in the range above about 1 GHz. Of course, the use of an absorber does not eliminate shadowing effects due to the human body so that these statements are valid only for directions of incidence from the half-space in front.

Fig. 9 shows the relative deviation of the maximum value of the electric and magnetic field strength as a function of frequency for the directions of incidence we studied. The maximum deviations lie between the "Max" and "Min" curves, and underestimating of the field exposure is practically impossible. For three directions of incidence, the maximum values are not representative in certain frequency ranges and are thus shown separately. In particular, for a vertical incidence of the wave from above and a polarization in the *x*-direction, an underestimation of the exposure of up to 6.5 dB occurs. However, it drops significantly with a small change in the direction of incidence or polarization.

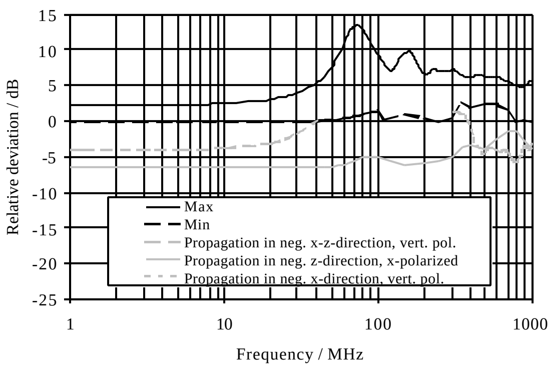

Fig. 9: Relative deviation of the maximum value of the electric and magnetic field strength for the directions of incidence investigated

4. Body Model with Arms bent

In the section above, the computed field conditions were described that exist in front of the body in the region of the chest pocket since it is customary to carry a field strength warning device there. However, other persons might hold the meter in their hand in front of the body, particularly when attempting to localize a radiation source. To compute the field conditions for this scenario, we used a modified body model with the arms bent, as shown in **Fig. 10** as FEKO simulation model.

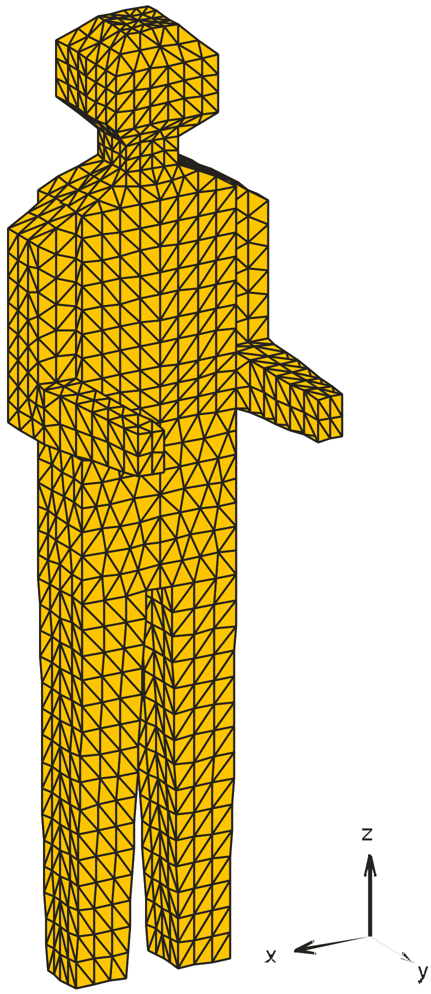

Fig. 10: FEKO simulation model for the body with arms bent

We will not present the results obtained with this model in great detail since the field conditions differ from those shown in Figs. 5-8 only in one area: Due to the greater distance between the field strength meter and the body, the effects of the body are smaller. Thereby, further reducing of the risk of underestimating the field exposure and also significantly decreasing the overestimation, particularly in the region of the halfwave resonance of the body, can be achieved.

5. Conclusion

For the computations we performed, the body was not modeled using a lossy dielectric, as might seem obvious at first; ideal conductivity was assumed. This is acceptable since we showed that the field conditions in front of the body can be described very well in this manner, although the effects of the body are somewhat overestimated. The simplifications offered by this approach were a prerequisite to our computations for enabling investigations of frequencies beyond 1 GHz.

The field conditions in front of the body models were considered for different directions of incidence with horizontal and vertical polarization of the incident planar wave. In the case of the halfwave resonance of the body (approx. 70 MHz in a free field), the electric and magnetic field strength are increased up to 13.5 dB. Below this resonant frequency, the electric and magnetic field are both increased up to 3 dB or attenuated up to 20 dB depending on the direction of incidence and polarization. The same is also true above the halfwave resonant frequency, where an increase of up to 10 dB occurs.

It is important to note that a strong attenuation of the electric field practically never coincides with a strong attenuation of the magnetic field at any given frequency. This means we must measure both fields simultaneously. By doing so, we eliminate the risk of underestimating the field exposure for almost all directions of incidence and polarizations we investigated. The field vectors are also altered in orientation as well as in magnitude, particularly in the region of the halfwave resonance, making it necessary to measure all of the field components.

If we measure just the electric or magnetic field in the vicinity of the body (as all of the existing warning devices do), a significant underestimation of the field exposure can be expected in many frequency ranges and directions of incidence.

A warning device and field strength meter that was developed based on the above insights is available commercially. The device ("ESM-20") is built by Wandel & Goltermann and uses isotropic electric and magnetic field sensors simultaneously. The risk of a significant underestimation of the exposure - a problem with warning devices that measure only the electric or magnetic field - is eliminated by the ESM-20. The wide frequency range from 1 MHz to 18 GHz (H field: up to 1 GHz) is another innovative feature. In the past, at least two meters were necessary to cover this range.

Bibliography

[1] R. RENO and D.E. BEISCHER: *Microwave Reflection, Diffraction and Transmission by Man*. Navel Aerospace Medical Research Laboratory, Pensacola, Florida, June 1973.

[2] U. JAKOBUS: *Erweiterte Momentenmethode zur Behandlung kompliziert aufgebauter und elektrisch großer elektromagnetischer Streuprobleme*. Dissertation, Universität Stuttgart, published as Fortschritts-Berichte VDI, Vol. 21: Elektrotechnik, 171, VDI-Verlag, 1995.

* [2] the title would be in English:
Extended method of moments for the treatment of complicated and electrically large electromagnetic scattering problems.

This paper was first published under the same title in “Frequenz 52 (1998), 9 – 10“.

Fig. 5 in the original publication was not correct.